JOURNAL OF APPLIED POLYMER SCIENCE VOL. 19, 3257–3276 (1975)

Studies on Blown Film Extrusion. I. Experimental Determination of Elongational Viscosity

CHANG DAE HAN and JONG YOO PARK, *Department of Chemical Engineering, Polytechnic Institute of New York, Brooklyn, New York, 11201*

Synopsis

Blown-film extrusion experiments were carried out to investigate the elongational flow behavior of viscoelastic polymer melts at different melt temperatures. Materials chosen for study were high-density polyethylene, low-density polyethylene, and polypropylene. In the study, isothermal blown-film extrusion experiments were carried out in which the molten blown film traveled upward through a heated chamber of about 13 in. in length maintained at the same temperature as the melt. Axial tension was measured at the take-up roller, the axial profiles of bubble diameter were determined by a photographic technique, and, from the samples collected, the variation in the film thickness along the axial direction was found. These measurements were used later to determine the elongational viscosity, using the force balance equations. It was found, in the experiment, that a careful control of the pressure difference across the thin film permitted one to maintain the bubble diameter constant, and, therefore, depending on the choice of the extrusion conditions, either a uniaxial or biaxial elongational flow was made possible. The experimental results show that, depending on the materials, elongation rate, and melt temperature tested, the elongational viscosity may decrease or increase with elongation rate, and may also stay constant independent of elongation rate. It was observed that the data of elongational viscosity obtained under uniaxial stretching in blown film extrusion is consistent with the data of elongational viscosity obtained earlier by use of the melt-spinning operation.

INTRODUCTION

In recent years, the blown film process has attracted great interest in the polymer processing industry for the production of thin thermoplastic films and is the source, today, of much of the polyolefin film, poly(vinyl chloride) film, and poly(vinylidiene chloride) (saran) film sold.[1]

As schematically shown in Figure 1, in the blown film process a thin film is produced by means of the extrusion of a polymer melt through an annular die. The molten polymer tube exiting from the die is drawn upward by a take-up device. At the bottom of the die, air is introduced, inflating the tube to form a bubble. An air ring is also used to rapidly cool the hot bubble and solidify it at some distance above the die exit. The inflated, solidified bubble is then flattened as it passes through the nip rolls. The nip rolls, driven by a variable-speed motor, provide the axial tension needed to pull the film upward, and they form an air-tight seal so that a constant pressure, slightly above atmospheric, is maintained in the inflated bubble. The pressure inside the bubble is controlled by adjusting the air supply to the bottom of the die.

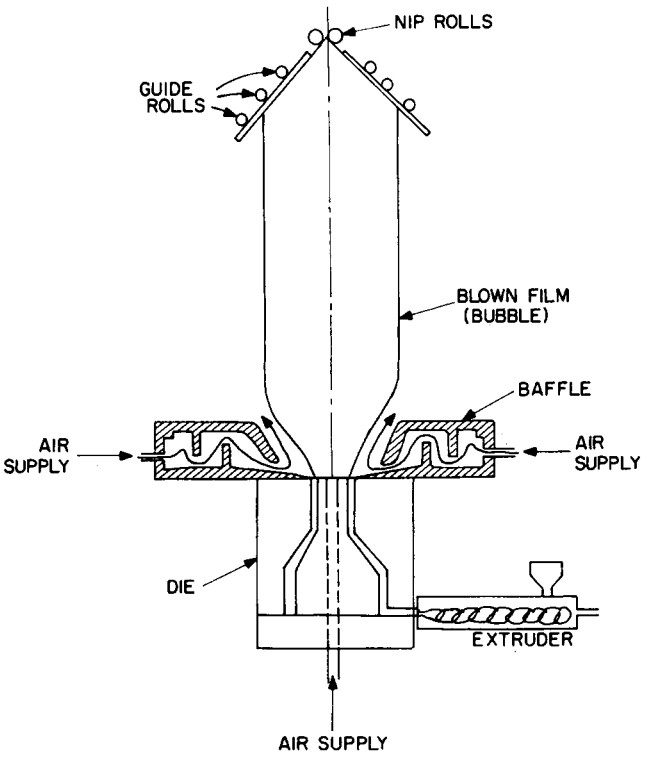

Fig. 1. Schematic of the blown film process.

In the past, however, very little attention has been given to the blown film process from a fundamental level, except for the theoretical attempt made by Pearson[2] and Pearson and Petrie.[3,4] As may be surmised, a better control of the blown film process requires a better understanding of the problems involved with elongational flow. As in fiber spinning, the polymer melt exiting from the die flows under a mechanical tension in the direction of flow. However, in the blown film process, the tube of molten polymer is extended in both the transverse and the axial (machine) directions, as described above in reference to Figure 1. Therefore, rheologically speaking, the blown film process should be treated from the point of view of biaxial elongational flow, whereas the fiber spinning process may be treated from the point of view of uniaxial elongational flow.

In recent years, several researchers[5–9] have studied the elongational flow encountered in fiber spinning. The primary objective of these studies was to experimentally determine the elongational viscosity involved with the melt spinning[5,6,7] and wet spinning[8,9] processes.

However, to the best knowledge of the authors, there has been no study reported in the literature which treated the blown film process from the point of view of elongational flow. Having recognized the importance of the problem from both the practical and fundamental points of view, the authors have recently embarked on a systematic investigation of the blown film process, both theoretically and experimentally.

The purpose of this paper, the first of the series, is to report our study of the experimental determination of the elongational viscosity of polymer melts in the blown film process. Both uniaxial and biaxial elongational flows were investigated by carefully controlling the pressure difference between the inside and the outside of a thin blown film. In subsequent papers, we shall present an analysis of the deformation and heat transfer problems involved in the blown film process, flow instabilities frequently encountered in blown film extrusion, and, also, the mechanical properties and the molecular orientation of the finished film as affected by different processing conditions.

EXPERIMENTAL

Apparatus and Experimental Procedure

The apparatus consisted of a 1-in. Killion extruder, an annular die, an isothermal chamber, nip rolls (driven by a variable-speed motor and located at about 6 ft above the die exit), and a take-up device. Figure 2 shows a picture of the apparatus. The compressed air for inflating the bubble was introduced at the bottom of the die.

In the experiment, an isothermal chamber with a glass window about 13 in. long was attached to the die exit, and the temperature of the air in the chamber was controlled, together with those of other pieces of equipment (the extrusion die and feed lines), by thermistor-operated thermal regulators. The air in the isothermal chamber was maintained at the same temperature as the polymer melt so that no cooling of the blown bubble would occur in it. The isothermal experiment was carried out in order to eliminate the temperature effect on the deformation of the bubble. The effect of temperature was investigated by running isothermal experiments at various melt temperatures. The actual temperatures chosen for the experiment varied from material to material, as will be discussed later.

In the experiment, the shape of the bubble was photographed at each extrusion condition, and the tension was measured using a Tensitron tensiometer (Model 5A) at a point just below the nip rolls. After photographing the bubble, the sample was collected and cooled. The samples were later used to measure the distribution of film thickness along the machine direction. The air pressure was measured by a water manometer and controlled with a regulating valve. The mass flow rate of the melt was determined by collecting the extrudate for a predetermined interval, and the average linear velocity of the melt at the die exit was determined from the measured mass flow rate, the density of the melt, and the opening and diameter of the annular die. Figure 3 gives a schematic of the annular die used for the experiment. It has two feed ports so that the melt from the extruder flows uniformly upward. In order to improve the uniform flow in the annular space, shallow grooves were provided at the converging section of the die.

Materials

The materials used were high-density polyethylene (HDPE) (DMDJ 5140, Union Carbide), low-density polyethylene (LDPE) (PEP 211, Union Car-

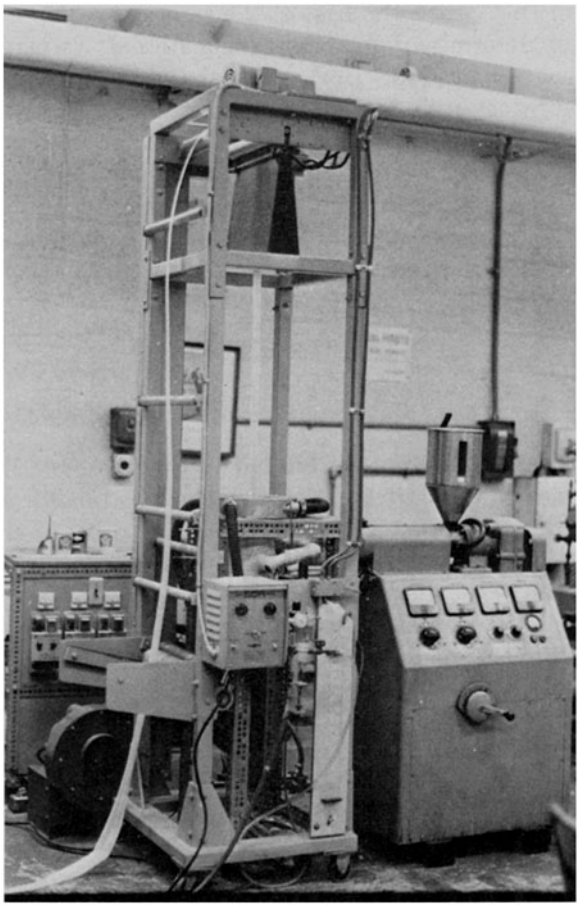

Fig. 2. Picture of the apparatus.

bide), and polypropylene (PP) (E 115, Exxon Chemical). The choice of these materials was based on the fact that Han and his co-workers[6,10,11] had already extensively measured the shear viscosity in capillary flow, the elongational viscosity in melt spinning, and the molecular characteristics of these materials in previous research programs.

THEORETICAL CONSIDERATION OF THE ELONGATIONAL FLOW IN BLOWN FILM EXTRUSION

The Rate of Strain Tensor

We focus our attention at the region where both the bubble diameter a and the film thickness h vary with the machine direction z. Now, in order to express the velocity gradients in terms of a, h, and z, we shall follow the approach taken by Pearson and Petrie,[3,4] who used the theory of thin shells as an approximation. This approximation assumes that the film thickness h is small compared with other dimensions of the bubble and its radii of curvature (i.e., $h \ll a$), permitting one to approximate the *curved* film by a *plane* film.

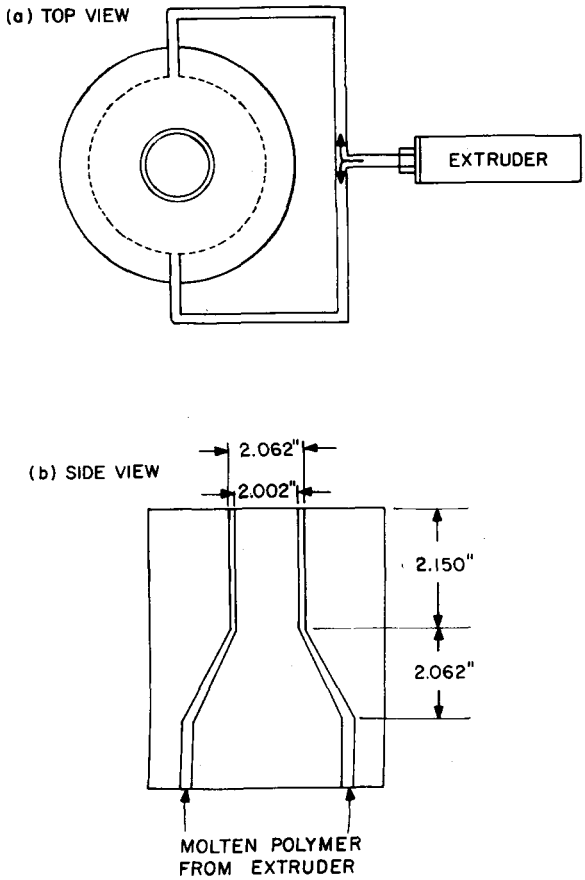

Fig. 3. Schematic of the annular die used.

Consider the coordinates shown in Figure 4. Our task is to relate the cylindrical coordinates (ρ, Φ, z) with the rectangular Cartesian coordinates (ξ_1, ξ_2, ξ_3) at a point P on the surface of the film. Note that ξ_1 is in the direction of flow (tangent to the film), ξ_2 is normal to the film, and ξ_3 is in the transverse (circumferential) direction. Let (v_1, v_2, v_3) be velocity components in the coordinates (ξ_1, ξ_2, ξ_3). Now, the rate-of-strain tensor $\mathbf{e}$ may be written as

$$\mathbf{e} = \begin{Vmatrix} e_{11} & 0 & 0 \\ 0 & e_{22} & 0 \\ 0 & 0 & e_{33} \end{Vmatrix} \tag{1}$$

in which e_{11}, e_{22}, and e_{33} are defined by

$$e_{11} = \frac{\partial v_1}{\partial \xi_1}, \quad e_{22} = \frac{\partial v_2}{\partial \xi_2}, \quad e_{33} = \frac{\partial v_3}{\partial \xi_3}. \tag{2}$$

It should be noted that, in eq. (1), the film is assumed to be almost plane, and consequently shear components of the rate of strain are assumed to be negligible.

Note that e_{22} and e_{33} may be represented in terms of a and h as a function of z[3]:

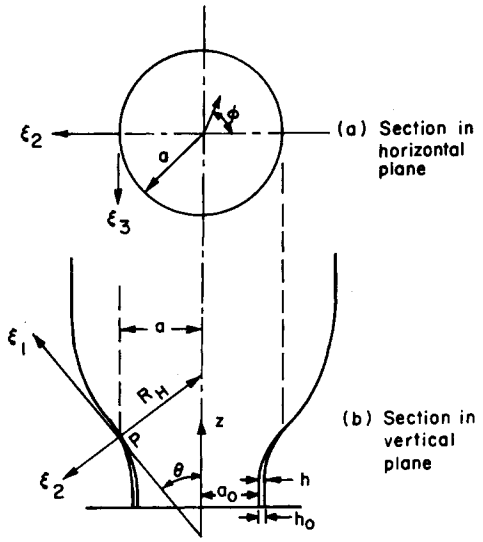

Fig. 4. Coordinate systems describing the deformation of a bubble.

$$e_{22} = \frac{1}{h}\frac{dh}{dt} = \frac{1}{h}\frac{dh}{d\xi_1}\frac{d\xi_1}{dt} = v_1 \cos\theta \frac{1}{h}\frac{dh}{dz} \tag{3}$$

$$e_{33} = \frac{1}{a}\frac{da}{dt} = \frac{1}{a}\frac{da}{d\xi_1}\frac{d\xi_1}{dt} = v_1 \cos\theta \frac{1}{a}\frac{da}{dz}. \tag{4}$$

Since the equation of continuity gives

$$e_{11} + e_{22} + e_{33} = 0 \tag{5}$$

e_{11} may be expressed in terms of a and h by

$$e_{11} = -(e_{22} + e_{33}) = -v_1 \cos\theta\left(\frac{1}{h}\frac{dh}{dz} + \frac{1}{a}\frac{da}{dz}\right). \tag{6}$$

Since v_1 can be expressed in terms of the flow rate Q, a, and h by

$$\frac{d\xi_1}{dt} = v_1 = \frac{Q}{2\pi ah} \tag{7}$$

eqs. (3), (4), and (6) may be rewritten as

$$e_{11} = -\frac{Q\cos\theta}{2\pi ah}\left(\frac{1}{a}\frac{da}{dz} + \frac{1}{h}\frac{dh}{dz}\right) \tag{8}$$

$$e_{22} = \frac{Q\cos\theta}{2\pi ah^2}\frac{dh}{dz} \tag{9}$$

$$e_{33} = \frac{Q\cos\theta}{2\pi a^2 h}\frac{da}{dz}. \tag{10}$$

Substituting eqs. (8)–(10) into eq. (1), we obtain:

$$\mathbf{e} = \frac{Q\cos\theta}{2\pi ah}\begin{Vmatrix} -\left(\frac{1}{a}\frac{da}{dz} + \frac{1}{h}\frac{dh}{dz}\right) & 0 & 0 \\ 0 & \frac{1}{h}\frac{dh}{dz} & 0 \\ 0 & 0 & \frac{1}{a}\frac{da}{dz} \end{Vmatrix}. \tag{11}$$

Let us now consider a few special cases of eq. (11).

Special Case 1. Uniform biaxial stretching. For uniform biaxial stretching, we have

$$e_{11} = e_{33}, \quad e_{22} = -2e_{11} = -2e_{33}. \tag{12}$$

Using eqs. (8)–(10) in eq. (12), we obtain

$$e_{11} = e_{33} = \frac{Q\cos\theta}{2\pi a^2 h}\frac{da}{dz} = -\frac{Q\cos\theta}{4\pi ah^2}\frac{dh}{dz} \tag{13}$$

$$e_{22} = -\frac{Q\cos\theta}{\pi a^2 h}\frac{da}{dz} = \frac{Q\cos\theta}{2\pi ah^2}\frac{dh}{dz}. \tag{14}$$

Therefore, the rate-of-strain tensor may be represented as

$$\mathbf{e} = \frac{Q\cos\theta}{2\pi a^2 h}\frac{da}{dz}\begin{Vmatrix} 1 & 0 & 0 \\ 0 & -2 & 0 \\ 0 & 0 & 1 \end{Vmatrix} = -\frac{Q\cos\theta}{4\pi ah^2}\frac{dh}{dz}\begin{Vmatrix} 1 & 0 & 0 \\ 0 & -2 & 0 \\ 0 & 0 & 1 \end{Vmatrix}. \tag{15}$$

Special Case 2. Uniaxial stretching. For uniaxial stretching, we have

$$e_{22} = e_{33}, \quad e_{11} = -2e_{22} = -2e_{33}. \tag{16}$$

Using eqs. (8)–(10) in eq. (16), we obtain

$$e_{11} = -\frac{Q\cos\theta}{\pi a^2 h}\frac{da}{dz} = -\frac{Q\cos\theta}{\pi ah^2}\frac{dh}{dz} \tag{17}$$

$$e_{22} = e_{33} = \frac{Q\cos\theta}{2\pi a^2 h}\frac{da}{dz} = \frac{Q\cos\theta}{2\pi ah^2}\frac{dh}{dz}. \tag{18}$$

Therefore, the rate-of-strain tensor may be represented as

$$\mathbf{e} = -\frac{Q\cos\theta}{2\pi a^2 h}\frac{da}{dz}\begin{Vmatrix} 2 & 0 & 0 \\ 0 & -1 & 0 \\ 0 & 0 & -1 \end{Vmatrix} = -\frac{Q\cos\theta}{2\pi ah^2}\frac{dh}{dz}\begin{Vmatrix} 2 & 0 & 0 \\ 0 & -1 & 0 \\ 0 & 0 & -1 \end{Vmatrix}. \tag{19}$$

Expressions of Elongational Viscosity

The total stress component T_{ij} may be given by

$$T_{ij} = -p\delta_{ij} + \tau_{ij} \quad (i, j = 1, 2, 3) \tag{20}$$

in which p denotes the isotropic pressure, δ_{ij} denotes the Kronecker delta, and τ_{ij} denotes deviatoric stresses.

Referring to Figure 4, the fact that the stress at the free surface is equal to atmospheric pressure gives

$$T_{22} = 0. \tag{21}$$

Using eq. (21) in eq. (20), we obtain

$$p = \tau_{22}. \tag{22}$$

For convenience, we define the elongational viscosity η_B in blown film extrusion in general, as

$$\tau_{ij} = \eta_B(\Pi)e_{ij} \quad (i, j = 1, 2, 3) \tag{23}$$

in which Π is the second invariant of the rate-of-strain tensor **e**, defined as

$$\Pi = (e_{11}^2 + e_{22}^2 + e_{33}^2). \tag{24}$$

Using eq. (22) in eq. (20), we obtain

$$T_{11} = \tau_{11} - \tau_{22} \tag{25}$$

$$T_{33} = \tau_{33} - \tau_{22} \tag{26}$$

in which T_{11} is the tensile stress in the direction of flow and T_{33} in the transverse direction (i.e., the hoop stress). Substituting eq. (23) into eqs. (25) and (26), we get

$$T_{11} = \eta_B(\Pi)(e_{11} - e_{22}) \tag{27}$$

and

$$T_{33} = \eta_B(\Pi)(e_{33} - e_{22}) \tag{28}$$

respectively.

Therefore, the elongational viscosity in nonuniform biaxial stretching may be represented as

$$\eta_B(\Pi) = \frac{T_{11}}{e_{11} - e_{22}} \tag{29}$$

or

$$\eta_B(\Pi) = \frac{T_{33}}{e_{33} - e_{22}} \tag{30}$$

in which e_{11}, e_{22}, and e_{33} are given by eqs. (8), (9), and (10), respectively.

For uniform biaxial stretching, we have

$$T_{11} = T_{33}, \quad T_{22} = 0. \tag{31}$$

Hence, from eqs. (12), (27), (28), and (31), it follows that

$$\eta_B(\Pi) = \frac{T_{11}}{e_{11} - e_{22}} \tag{32}$$

in which e_{11} and e_{22} are given by eqs. (13) and (14), respectively.

For uniaxial stretching, we have

$$T_{22} = T_{33} = 0. \tag{33}$$

Hence, from eqs. (16), (27), (28), and (33) it follows that

$$\eta_B(\Pi) = \frac{T_{11}}{e_{11} - e_{22}} \tag{34}$$

in which e_{11} and e_{22} are given by eqs. (17) and (18), respectively.

If we define the elongational viscosity in the usual way by

$$\eta_E(\Pi) = \frac{T_{11}}{e_{11}} \tag{35}$$

then we find the following relationships:

(i) For uniform biaxial stretching, from eqs. (32) and (35), we have

$$\eta_E(\Pi) = 3\eta_B(\Pi) = \frac{3T_{11}}{e_{11} - e_{22}} \tag{36}$$

(ii) For uniaxial stretching, from eqs. (34) and (35), we have

$$\eta_E(\Pi) = (3/2)\eta_B(\Pi) = \frac{3T_{11}}{2(e_{11} - e_{22})}. \tag{37}$$

If we now consider a very special case of eq. (23), namely, the Newtonian fluid, eq. (23) can be rewritten as

$$\tau_{ij} = 2\eta_0 e_{ij} \tag{38}$$

i.e.,

$$\eta_B = 2\eta_0. \tag{39}$$

Then, from eqs. (36) and (39), we have

$$\eta_E = 6\eta_0 \tag{40}$$

for uniform biaxial stretching, and from eqs. (37) and (39), we have

$$\eta_E = 3\eta_0 \tag{41}$$

for uniaxial stretching. It is interesting to note that eq. (40) was discussed in a recent paper by Denson[12] and that eq. (41) was discussed by a number of investigators since the original work by Trouton.[13]

Method of Determining the Elongational Viscosity in Blown Film Extrusion

If one wishes to determine the elongational viscosity in the blown film process, one may use eq. (29), or eq. (30), for nonuniform biaxial stretching, eq. (32) for uniform biaxial stretching, and eq. (34) for uniaxial stretching. For this, one has to take measurements of a, h, and θ as a function of z, and the axial tension T_{11}.

Referring to the coordinate systems given in Figure 4, a force balance on the film may be written as

$$2\pi a \cos\theta P_L + \pi\Delta P(A^2 - a^2) + 2\pi\rho g \int_z^Z ah \sec\theta dz = F_Z \tag{42}$$

in which a and A are bubble radii at z and Z (the frost line), h is the film thickness at z, P_L is the force acting in the direction of flow (i.e., machine direction), ΔP is the pressure difference across the film, ρ is the density of a melt, g is the gravitational acceleration, and F_Z is the tensile force at $z = Z$ (i.e., at the frost line). As described above, since the tension is measured at a point near the nip rolls, say, $z = L$, F_Z is represented by

$$F_Z = F_L - 2\pi\rho_s g A H(L - Z) \tag{43}$$

in which F_L is the tension actually measured at $z = L$, ρ_s is the density of a solid film, A is the bubble radius at $z = Z$, and H is the film thickness at $z = Z$.

In the region where the bubble is being blown (i.e., between $z = 0$ and $z = Z$), the force in the transverse direction P_H and the tensile force P_L are balanced by ΔP[3,4]:

$$\Delta P = \frac{P_L}{R_L} + \frac{P_H}{R_H} - \rho g h \sin\theta \tag{44}$$

where R_L and R_H are the principal radii of curvature of the film, given by

$$R_H = a/\cos\theta \tag{45}$$

$$R_L = -\left[1 + \left(\frac{da}{dz}\right)^2\right]^{3/2} \Big/ \frac{d^2a}{dz^2} = -\sec^3\theta \Big/ \frac{d^2a}{dz^2}. \tag{46}$$

On the other hand, P_L and P_H may be given by[3,4]

$$P_L = \int_0^h T_{11} d\xi_2 = hT_{11} \tag{47}$$

$$P_H = \int_0^h T_{33} d\xi_2 = hT_{33}. \tag{48}$$

Substituting eq. (47) into the left-hand side of eq. (42), and eq. (43) into the right-hand side of eq. (42), we obtain

$$T_{11} = \frac{F_R}{2\pi a h \cos\theta} \tag{49}$$

in which

$$F_R = F_L - \pi\Delta P(A^2 - a^2) - 2\pi\rho g \int_z^Z ah \sec\theta \, dz - 2\pi\rho_s g A H(L - Z). \tag{50}$$

Now, it can be seen that once measurements of a, h, and θ are taken as a function of z, use of eq. (50) in eq. (49) permits one to calculate the tensile stress T_{11} and hence the elongational viscosity η_B for nonuniform biaxial stretching using eq. (29), together with eqs. (8) and (9).

Similarly, eq. (36) may be used to calculate the elongational viscosity η_E for *uniform* biaxial stretching, with the aid of eqs. (13), (14), (32), (49), and (50). Also, the elongational viscosity η_E for *uniaxial* stretching (i.e., $\Delta P = 0$) can be calculated using eqs. (17), (18), (34), (49) and (50).

RESULTS AND DISCUSSION

Bubble Shape as Affected by Processing Conditions

Representative bubble shapes are given in Figure 5 for high-density polyethylene and in Figure 6 for low-density polyethylene. Hundreds of pictures were taken at various extrusion conditions, but the limitation of space does

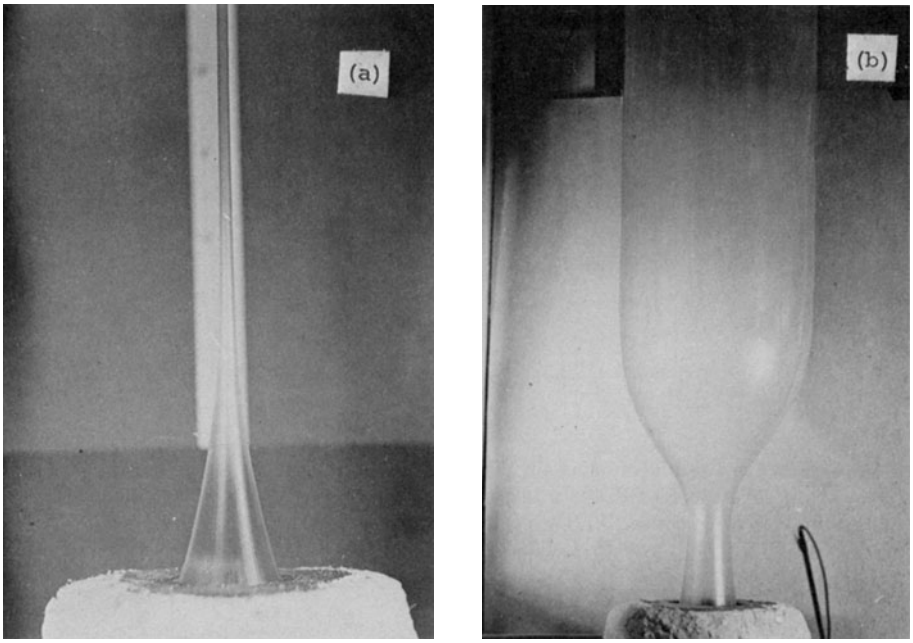

Fig. 5. Bubble shapes of high-density polyethylene at 200°C: (a) uniaxial stretching (Δp = 0): Q = 6.97 g/min, V_0 = 0.1226 cm/sec, V_L/V_0 = 112.39; (b) biaxial stretching ($\Delta P = 1.16 \times 10^{-2}$ psi): Q = 20.93 g/min, V_0 = 0.378 cm/sec, V_L/V_0 = 36.46.

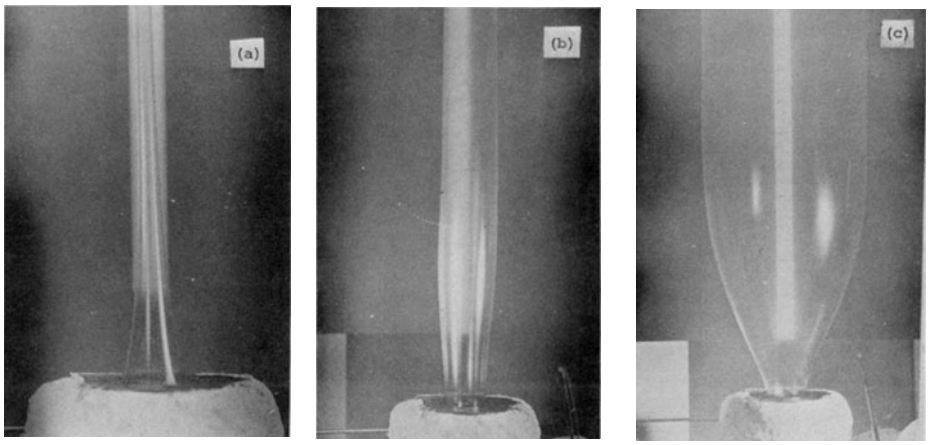

Fig. 6. Bubble shapes of low density polyethylene (T = 200°C) at extrusion conditions: (a) Δp = 0, Q = 9.15 g/min, V_0 = 0.174 cm/sec, V_L/V_0 = 79.4; (b) $\Delta p = 1.09 \times 10^{-2}$ psi, Q = 18.1 g/min, V_0 = 0.346 cm/sec, V_L/V_0 = 28.9; (c) $\Delta p = 0.798 \times 10^{-2}$ psi, Q = 18.1 g/min, V_0 = 0.346 cm/sec, V_L/V_0 = 28.9.

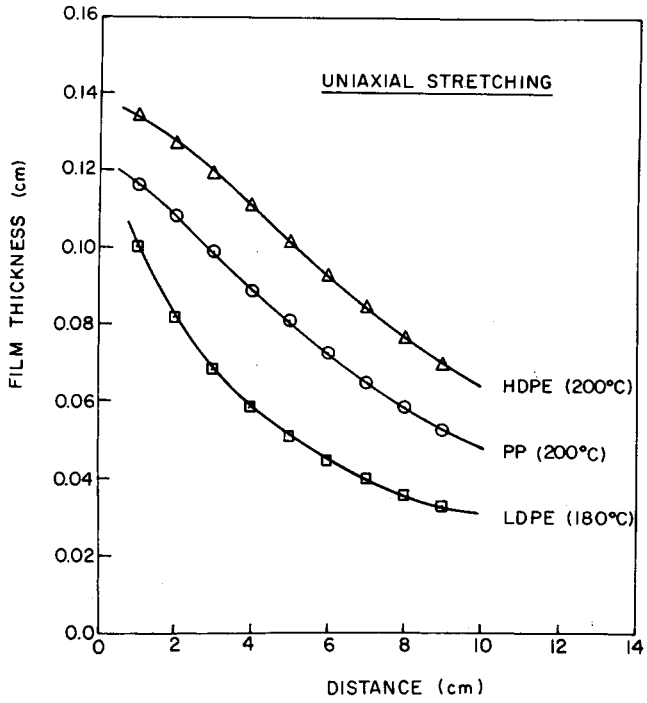

Fig. 7. Thickness profile of uniaxially stretched films: for HDPE, Q = 7.0 g/min, V_0 = 0.126 cm/sec, V_L/V_0 = 109.6; for PP, Q = 9.15 g/min, V_0 = 0.174 cm/sec, V_L/V_0 = 79.4; for LDPE, Q = 7.20 g/min, V_0 = 0.134 cm/sec, V_L/V_0 = 129.5.

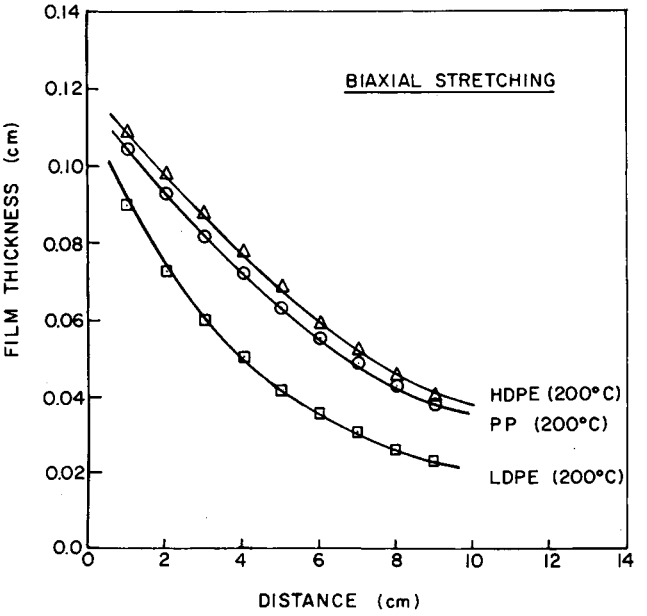

Fig. 8. Thickness profile of biaxially stretched films: for HDPE, Q = 20.9 g/min, V_0 = 0.377 cm/sec, V_L/V_0 = 36.7, Δp = 0.0051 psi; for PP, Q = 13.88 g/min, V_0 = 0.259 cm/sec, V_L/V_0 = 67.2, Δp = 0.0051 psi; for LDPE, Q = 18.10 g/min, V_0 = 0.346 cm/sec, V_L/V_0 = 28.9, Δp = 0.0058 psi.

not permit us to present many here. It was observed that the bubble shape was extremely sensitive to the variation in air pressure within the bubble. As may be expected, bubbles of different shapes give rise to films of different thicknesses. For a fixed flow rate, the take-up speed was found, also, to be a very sensitive variable affecting the film thickness. Of course, a meaningful variable would be the stretch ratio V_L/V_0, which is defined as the ratio of the linear velocity at the take-up device to the average linear velocity of the melt at the die exit.

Representative profiles of film thickness are given in Figure 7 for uniaxially stretched films, and in Figure 8 for biaxially stretched films. Note that extrusion conditions are almost identical in the two cases, except for the air pressure within the bubble. It is seen in these figures that biaxial stretching gives rise to thinner films than uniaxial stretching, as would be expected. It may be pointed out also that the mechanical properties of a film would be different, depending on whether the film is uniaxially or biaxially stretched. This is because molecular orientation would be different for the two different types of stretching. This subject will be dealt with in a future publication.

Elongational Flow Behavior

Having measured the bubble radius a, film thickness h, and the angle θ as functions of machine direction z, we were able to calculate the elongation rate

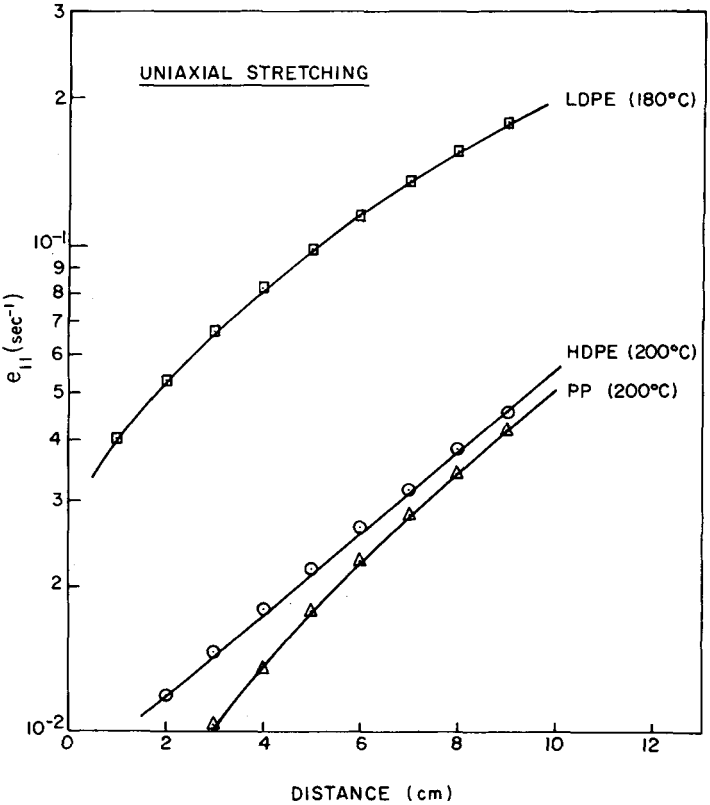

Fig. 9. Profiles of elongation rate in the machine direction in uniaxial stretching ($\Delta p = 0$). Extrusion conditions same as in Fig. 7.

at different values of z. Figure 9 gives plots of elongation rate versus axial distance for uniaxial stretching ($\Delta P = 0$), and Figure 10 gives the same for biaxial stretching ($\Delta P \neq 0$). Note that eq. (17) was used to calculate the

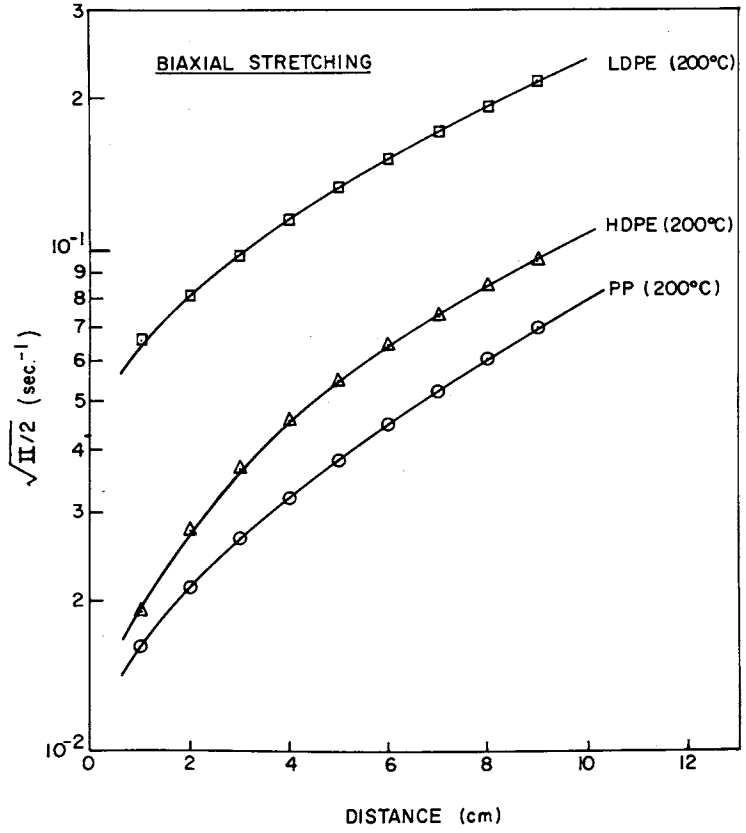

Fig. 10. Profiles of elongation rate in the machine direction in biaxial stretching. Extrusion conditions same as in Fig. 8.

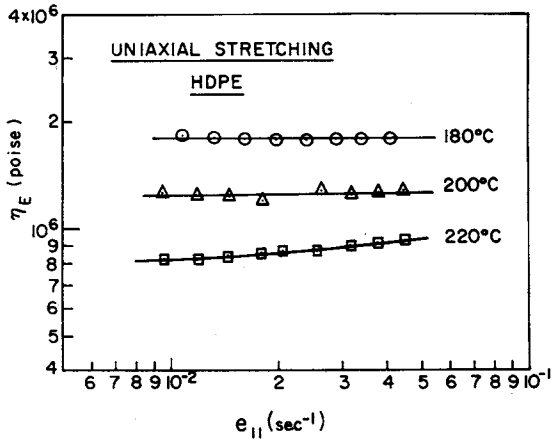

Fig. 11. Elongational viscosity vs. elongation rate for high-density polyethylene in uniaxial stretching: $Q = 7.0$ g/min, $V_0 = 0.126$ cm/sec, $V_L/V_0 = 109.6$, $\Delta p = 0$.

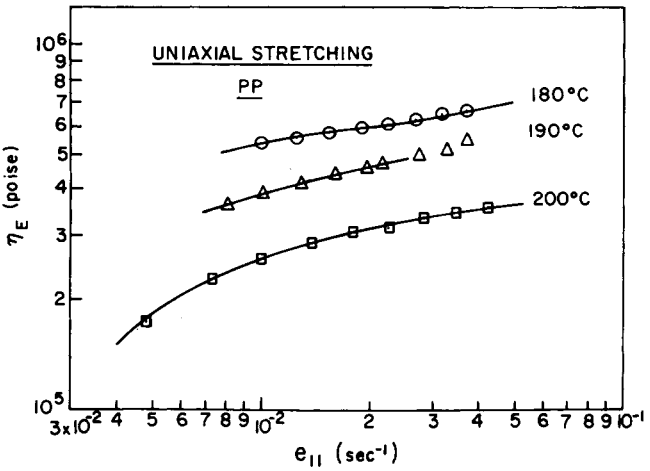

Fig. 12. Elongational viscosity vs. elongation rate for polypropylene in uniaxial stretching: Q = 7.2 g/min, V_0 = 0.134 cm/sec, V_L/V_0 = 129.5, Δp = 0.

elongation rate for uniaxial stretching, but that the elongation rate for biaxial stretching was calculated using the following expression:

$$\sqrt{\Pi/2} = \frac{Q \cos\theta}{2\pi ah}\left[\left(\frac{1}{a}\frac{da}{dz}\right)^2 + \left(\frac{1}{a}\frac{da}{dz}\right)\left(\frac{1}{h}\frac{dh}{dz}\right) + \left(\frac{1}{h}\frac{dh}{dz}\right)^2\right]^{1/2} \quad (51)$$

which is obtained from eq. (24) using eqs. (8)–(10). It is seen in Figures 9 and 10 that elongation rate increases with axial distance (i.e., machine direction z). In other words, constant values of elongation rate do not prevail in this method of film manufacture. Note that a similar observation was reported earlier by Han and Lamonte,[6] who were then investigating the melt-spinning process.

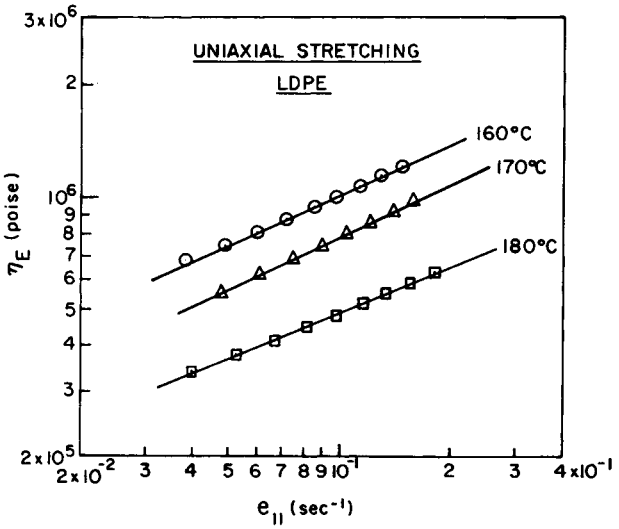

Fig. 13. Elongational viscosity vs. elongation rate for low-density polyethylene in uniaxial stretching: Q = 9.15 g/min, V_0 = 0.174 cm/sec, V_L/V_0 = 79.4, Δp = 0.

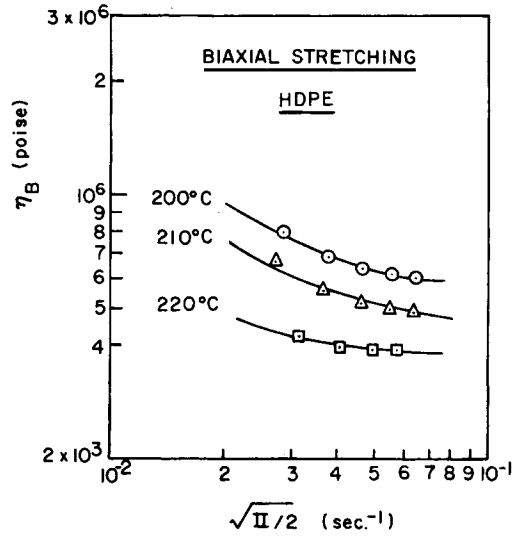

Fig. 14. Elongational viscosity vs. elongation rate for high-density polyethylene in biaxial stretching: Q = 20.93 g/min, V_0 = 0.377 cm/sec, V_L/V_0 = 36.7, Δp = 0.0109 psi.

Plots of elongational viscosity versus elongation rate in uniaxial stretching ($\Delta p = 0$) are given in Figure 11 for high-density polyethylene, in Figure 12 for polypropylene, and in Figure 13 for low-density polyethylene. Also, plots of elongational viscosity versus elongation rate in biaxial stretching ($\Delta p \neq 0$) are given in Figure 14 for high-density polyethylene, in Figure 15 for polypropylene, and in Figure 16 for low-density polyethylene. It is worth pointing out that in all experimental runs only *nonuniform* biaxial stretching (i.e., $e_{11} \neq e_{33}$) was observed.

It is seen in Figures 11 to 13 that, over the range of elongation rates investigated, in uniaxial stretching the elongational viscosity of high-density poly-

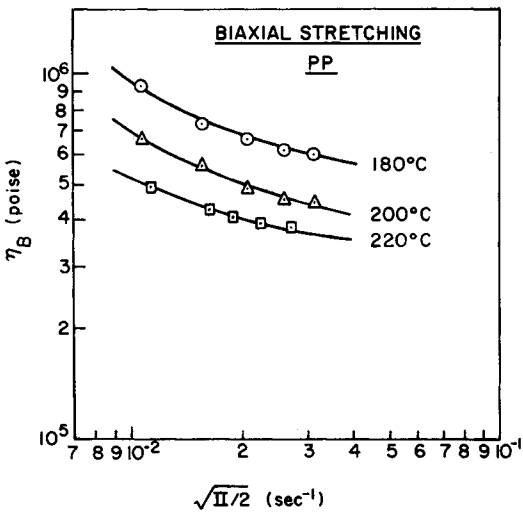

Fig. 15. Elongational viscosity vs. elongation rate for polypropylene in biaxial stretching: Q = 13.88 g/min, V_0 = 0.258 cm/sec, V_L/V_0 = 67.2, Δp = 0.0051 psi.

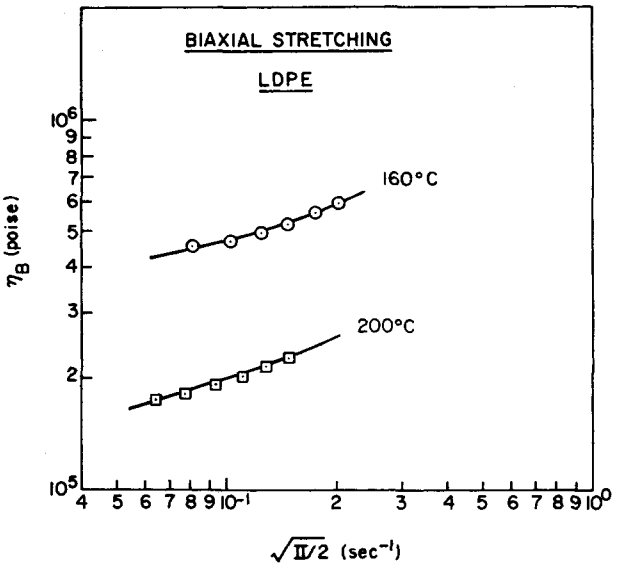

Fig. 16. Elongational viscosity vs. elongation rate for low-density polyethylene in biaxial stretching: Q = 18.10 g/min, V_0 = 0.346 cm/sec, V_L/V_0 = 28.9, Δp = 0.0058 psi.

ethylene stays constant at 180°C and 200°C but increases moderately with elongation rate at 220°C, whereas the elongational viscosities of polypropylene and low-density polyethylene increase with elongation rate at all three temperatures investigated. Note that for each material investigated, the range of melt temperature chosen for study was different. This was because, for instance, low-density polyethylene in the molten state could not support its weight within the isothermal chamber at temperatures above 180°C.

In biaxial stretching, however, Figures 14 to 16 show that over the range of elongation rates investigated the elongational viscosities of high-density polyethylene and polypropylene decrease with elongation rate, whereas the elongational viscosity of low-density polyethylene increases with elongation rate.

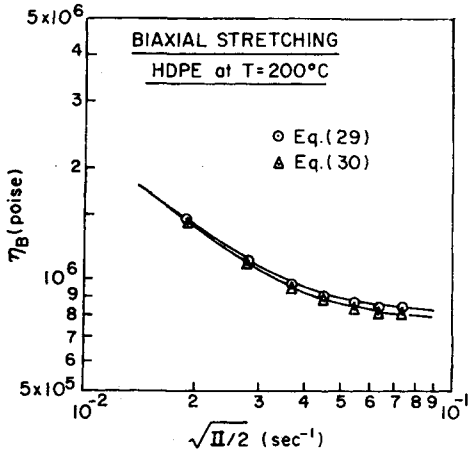

Fig. 17. Elongational viscosity vs. elongation rate for high-density polyethylene in biaxial stretching: Q = 20.93 g/min, V_0 = 0.377 cm/sec, V_L/V_0 = 36.7, Δp = 0.0109 psi.

It may be of interest to discuss more details of the experimental results presented above. First, the values of the measured tension range from 100 to 300 g, depending on the flow rate, the structure of polymer, and also the take-up speed. The tension accounted for by the weight of the polymer ranges somewhere between 10% and 20% of the total tension. This indicates the importance of the inclusion of gravitational effect in the total force balance equation given by eq. (50). It is estimated that the contribution of other components of force (e.g., the guide rolls and air drag) is small enough to be neglected (say, less than a few per cent of the total force).

Second, in biaxial stretching, the *apparent* elongational viscosity calculated either from eq. (29) or from eq. (30) should give identical values. Note that elongational viscosities plotted in Figures 14 to 16 are calculated using eq. (29). In order to use eq. (30), T_{33} must be calculated using eqs. (44) to (48), i.e.,

$$T_{33} = \frac{a}{h \cos \theta}\left(\Delta P + \frac{hT_{11}\dfrac{d^2a}{dz^2}}{\sec^3 \theta}\right) \tag{52}$$

It should be pointed out that in the derivation of eq. (52), the contribution of the term $\rho gh \sin \theta$, representing the gravity effect in eq. (44), was assumed to be negligible compared to that of other terms.

Figure 17 gives plots of η_B versus $\sqrt{\Pi/2}$ for biaxial stretching calculated using eqs. (29) and (30), respectively. Note that eq. (30) was used together with eq. (52). It may be said that agreement is reasonably good.

In recent years, Denson and his co-workers[12,14,15] have reported their measurements of biaxial elongational viscosity, showing that elongational viscosity decreases with elongation rate. It should be noted that Denson et al. restricted their experiments to *uniform* biaxial stretching, whereas the present study shows that the deformation was nonuniform biaxial stretching. As pointed out above, from the theoretical point of view the blown film process permits one to investigate *uniform* biaxial stretching, also. However, uniform biaxial stretching requires a unique relationship between the bubble radius and the film thickness, as eq. (13) demands. In the present study, however, satisfaction of the condition required by eq. (13) for uniform biaxial stretching was not met in all experimental runs. Of course, it was not our concern in this study, but even if we had wished to, it would not have been possible to run experiments guaranteeing *uniform* biaxial flow. This is because, *a priori,* one does not have information on the profiles of film thickness to permit one to control the bubble radius to satisfy eq. (13).

The range of elongation rates investigated by means of the bubble inflation technique[12,14,15] is a few orders of magnitude lower than that investigated in the present study by means of the blown film process. It is, also, interesting to note that the present study has not yielded constant elongation rate (see Figs. 9 and 10). From the practical standpoint, it is virtually impossible to control the elongation rate in processes such as in blown film extrusion and in melt spinning. In these processes, one is rather interested in controlling the stretch ratio V_L/V_0.

Finally, it may be of some interest to compare the elongational viscosity

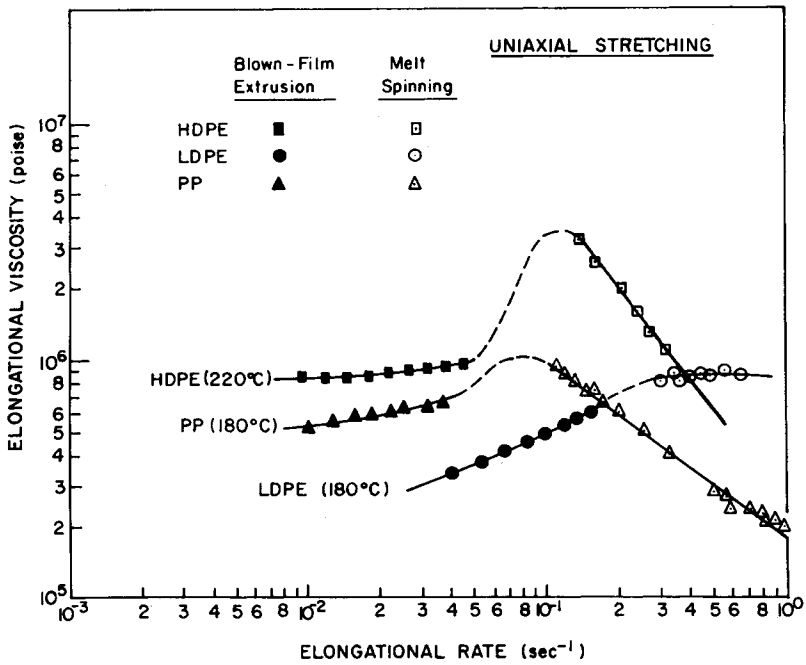

Fig. 18. Comparison of the elongational viscosities determined by means of the blown film process with those determined by means of the melt-spinning process.

determined by means of the blown film process with that determined by means of the melt spinning process. For this, the elongational viscosity data for uniaxial stretching given in Figures 11 through 13 above are compared with the melt spinning data.[6] A summary of the comparison is given in Figure 18.

A few observations are worth making. First, the elongation rates investigated in uniaxial stretching of the blown film process are lower than those investigated in the melt-spinning process. This is understandable in view of the fact that, in the former process, a molten polymer flows upward against the direction of the gravitational force, whereas, in the latter, it is quite the opposite. It appears that each experimental technique is limited to the range of elongation rates that can be investigated. Perhaps, it may be too much to expect that a particular experimental technique would permit one to have elongation rates over many decades. Second, considering the two entirely different experimental techniques employed, the correlation given in Figure 18 may be considered to be quite encouraging. Although data are lacking to justify the dotted lines in Figure 18, the overall shape of the elongational viscosity curves is in conformity with that recently hypothesized by Lamonte and Han[16] and also with a few theoretical predictions.[17,18]

CONCLUSIONS

It has been demonstrated that the blown film process can be used to study the elongational flow behavior of molten polymers. Unlike the melt-spinning process, the blown film process offers one the flexibility of studying uniaxial

stretching as well as biaxial stretching. It should be pointed out, however, that the theory, based on which various expressions of the rate of strain are derived, assumes that the curved film be approximated by a plane film. This approximation is justifiable when the film thickness is small compared with other dimensions of the bubble and its radii of curvature. As a matter of fact, the present experimental study appears to indicate that such an approximation is quite reasonable.

A number of specific conclusions may be drawn from the present study. First, elongation rate varies with machine direction (i.e., the direction of flow of a blown bubble). Second, elongational viscosity may increase, or decrease with elongation rate, or may stay constant independent of elongation rate, depending on the molecular structure of the materials and the range of elongation rates concerned. Third, elongational viscosity decreases with temperature, as expected. Fourth, the dependence of elongational viscosity on elongation rate in biaxial stretching may or may not be different from that in uniaxial stretching. Finally, comparison of the elongational viscosity determined by means of the blown film process with that determined by means of the melt-spinning process gives encouraging results.

References

1. W. R. R. Park, *Plastics Film Technology,* Van Nostrand Rheinhold Company, New York, 1969.
2. J. R. A. Pearson, *Mechanical Principles of Polymer Melt Processing,* Pergamon Press, London, 1966.
3. J. R. A. Pearson and C. J. S. Petrie, *J. Fluid Mech.*, **40**, 1 (1970); *ibid.*, **42**, 609 (1970).
4. J. R. A. Pearson and C. J. S. Petrie, *Plast. Polym.*, **38**, 85 (1970).
5. D. Acierno, J. N. Dalton, J. M. Rodriguez, and J. L. White, *J. Appl. Polym. Sci.*, **15**, 2395 (1965).
6. C. D. Han and R. R. Lamonte, *Trans. Soc. Rheol.*, **16**, 447 (1972).
7. I. Chen, G. E. Haggler, L. E. Abbott, J. N. Dalton, D. C. Bogue, and J. L. White, *Trans. Soc. Rheol.*, **16**, 473 (1972).
8. M. Zidan, *Rheol. Acta*, **8**, 89 (1969).
9. C. D. Han and L. Segal, *J. Appl. Polym. Sci.*, **14**, 2973 (1970).
10. C. D. Han and T. C. Yu, *J. Appl. Polym. Sci.*, **15**, 1149 (1971).
11. C. D. Han, *Trans. Soc. Rheol.*, **18**, 163 (1974).
12. D. D. Joye, G. W. Poehlein, and C. D. Denson, *Trans. Soc. Rheol.*, **17**, 287 (1973).
13. F. T. Trouton, *Proc. Roy. Soc. (London)*, **77**, 426 (1906).
14. C. D. Denson and R. J. Gallo, *Polym. Eng. Sci.*, **11**, 174 (1971).
15. D. D. Joye, G. W. Poehlein, and C. D. Denson, *Trans. Soc. Rheol.*, **16**, 421 (1972).
16. R. R. Lamonte and C. D. Han, *J. Appl. Polym. Sci.*, **16**, 3285 (1972).
17. R. I. Tanner, *Trans. Soc. Rheol.*, **12**, 155 (1968).
18. G. Marrucci, G. Titomanlio, and G. C. Sarti, *Rheol. Acta*, **12**, 269 (1973).

Received November 5, 1974
Revised April 21, 1975